

***In-situ* Observation on the Morphological Behavior of Bamboo under Flexural Stress with Respect to its Fiber-foam Composite Structure**

Meiling Chen, and Benhua Fei *

An *in-situ* observation on the morphological behavior of bamboo's fiber-foam composite structure under flexural stress was conducted, and the respective contribution of parenchymatous tissues and sclerenchyma fibers to the flexural ductility of bamboo was evaluated. Fibers or parenchymatous cells at the bottom suffered tensile stress during bending process, where initial microcracks occurred. The results suggested that the bottom parenchymatous tissues experienced a perforative tear along the loading direction, while fibers continued to stretch until several fibrous tensile failure cracks were observed. The subsequent crack growth mode was similar to that of the horizontal crack transmission that began when it reached fibers or somewhere between fibers, until another weak load-bearing point appeared, and then it expanded up through parenchymatous tissues. As a whole, the crack acted ladder-like in its growth, and the propagation paths were not restricted to a coherent one. Images of the morphological changes of the upper parenchymatous tissues and sclerenchyma fibers, which suffered compressive stress during bending process, indicated that parenchymatous tissues and sclerenchyma fibers made different contributions to the flexural ductility of bamboo. Sclerenchyma fibers supplied deformation resistance for bamboo's macroscopic deformation, while parenchymatous tissues offered deformation space due to the variation of cellular morphology and location.

Keywords: Bamboo; Parenchymatous tissue; Sclerenchyma fiber; Crack propagation; Flexural ductility

Contact information: International Centre for Bamboo and Rattan, No. 8 FuTong Eastern Avenue, Wangjing Area, Chaoyang District, Beijing, P. R. China, 100102;

* Corresponding author: feibenhua@icbr.ac.cn

INTRODUCTION

As one of the most significant non-wood renewable natural biomass materials in the world, bamboo possesses a functional gradient structure that can accommodate itself into complicated physiological activities and natural environments. Bamboo is a unidirectional fiber-foam biocomposite in which the sclerenchyma sheaths (fibers) of vascular bundles are embedded in porous parenchyma cells (foam) that contribute to the surprisingly lightweight-durable performance and flexural ductility of bamboo (Liese 1987; Aizenberg *et al.* 2005; Jiang 2007; Fratzi and Weinkamer 2007; Yu *et al.* 2014; Xian *et al.* 2015). To determine flexural ductility, a bending test was conducted by Obataya *et al.* (2007) towards split bamboo culm (*Phyllostachys pubescens*), and the results suggested that the bamboo allowed a large flexural deformation because its outer layer retains the tensile stress while the softer inner layer undergoes a large compressive deformation. It has been mentioned in multiple publications that the fiber-parenchyma combination and the seemingly optimal distribution of fibers improve the flexural ductility of bamboo (Obataya

et al. 2007; Abe and Yano 2010; Long *et al.* 2015); however, most studies have been limited to theories and concepts, rather than a direct observation of the bending process from the beginning of being loaded to the material's failure point.

Composites' failure behavior is a dynamic process in which the constitutional unit's structure gradually changes, and one or several failure modes occur jointly, until total failure of the composite. In this study, the dynamic morphological change inside of bamboo under flexural stress was investigated. The goal was to determine how the constitutional units, sclerenchyma fibers, and parenchyma cells in junction grant flexural ductility. In addition, the respective contribution of sclerenchyma fibers and parenchyma cells to the flexural ductility was considered based on high-resolution images captured during the bending process. The aim of this study was to provide a theoretical basis for the morphological and micro-mechanical behavior of bamboo, which would further make contributions to the bionic structure design of composites.

EXPERIMENTAL

Materials

Preparation

Four-year-old moso bamboo (*Phyllostachys pubescens*) was grown in Anji, Zhejiang Province, China. One-meter-length bamboo tube was obtained from the bottom of bamboo culm with a diameter at breast height (DBH) of no less than 100 mm, and bamboo slivers were processed into a size of 40 mm × 5.42 mm × 1.60 mm (length × width × thickness) along tangential direction from outer part by cutting machine. Each bamboo sliver was stored in a 23 °C conditioning chamber until an equilibrium moisture content of 8% to 12% was achieved.

Methods

Measurement

The flat and smooth surface of the bamboo sliver was obtained with a diamond cutter installed in a sliding microtome (M2000R; Leica Microsystems Inc., Wetzlar, Germany), and a 90 s gold sputtering (Deben UK Ltd., London, UK) was done towards the surface at vacuum ambiance (vacuum degree $\leq 10^{-2}$ mbar).

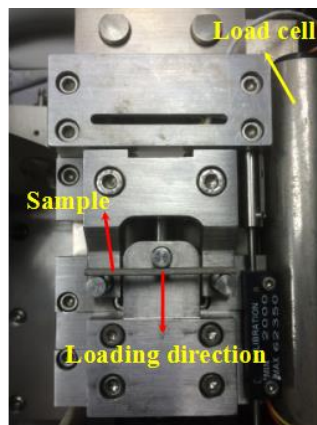


Fig. 1. *In-situ* SEM observation during the flexural test

The bamboo sliver was then put into the specimen chamber of a scanning electron microscope (Quanta2000; FEI Company, Hillsboro, OR, USA) and located at the central section of a three-point bending test jig of a Micro-tester (Deben UK Ltd., London, UK), as illustrated in Fig. 1. A voltage of 7.0 kV was discharged until the vacuum degree reached $5e^{-5}$. The span was 34 mm, and the loading speed was 0.2 mm/min. The morphological change of the sclerenchyma fibers and parenchyma cells were tracked and captured under a continuous micro-load.

RESULTS AND DISCUSSION

Compressed Parenchymatous Tissues on the Top

The morphological change of the parenchymatous tissues located on the top of the bamboo sliver specimen is illustrated in Fig. 2 during the bending process.

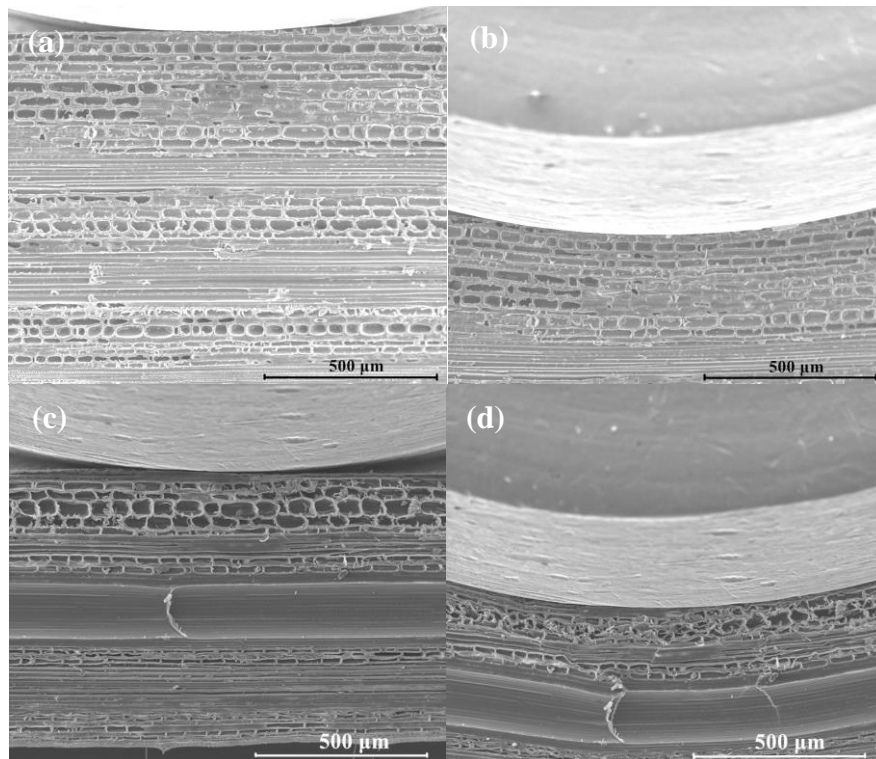


Fig. 2. Compressed parenchymatous tissues on the top

Notes: Fig. 2a and 2b are morphological images of the parenchymatous tissues located on the top of one specimen at the moment of 0 and 12 min upon loading, while Fig. 2c and 2d are the images for another specimen at the moment of 0 and 8 min.

Parenchymatous cells next to the squeeze head were rectangular and exhibited a vertical angle with the central axis before compression (Figs. 2a and 2c). As the compressive and flexural load increased, the orientation of the parenchymatous tissues changed, and an acute angle with a central axis arose. These cells turned oblate and flat from a rounded rectangle (Fig. 2b), and became highly compacted into a huddle (Fig. 2d), which indicated that the morphological change of the parenchymatous tissues offered space for the macroscopic deformation of the bamboo, and further made contributions to the

flexural ductility. It has also been documented in other research that the compressible nature of bamboo can be attributed to the parenchyma cells because bamboo consists of a large proportion of parenchyma cells (Obataya *et al.* 2007). In addition, no noticeable morphological change was found with respect to the fibers beneath those top parenchymatous tissues. This might be due to the interaction between components in bamboo, such that the parenchymatous ground tissue can pass stress loads and distribute the stress load onto the fibers (Shao *et al.* 2010).

Compressed Sclerenchyma Fibers on the Top

The sclerenchyma fibers on the top suffered compressive stress during the bending process. As presented in Fig. 3, the fiber cells were compacted along the fibrous diameters direction, and slippage and malposition occurred between the fibers. These effects were manifested as interfibrous cracks. Compressive stress was transferred to the parenchymatous tissues beneath those top sclerenchyma fibers. However, no obvious morphological changes were observed. The lack of change in appearance may have resulted from the “protective effect” of the upper fibers, rather than the neutral layer effect, because the location was far from the neutral layer. Such a “protective effect” implied a low elongation percentage at the break point for the fibers when compared to the deformation extent of the parenchymatous cells.

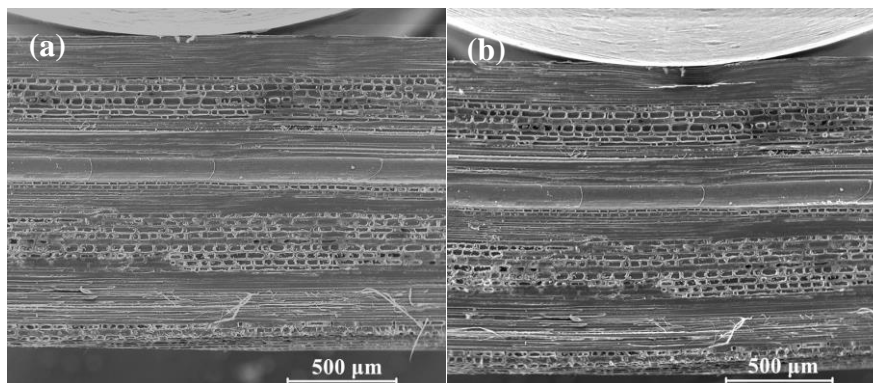


Fig. 3. Compressed sclerenchyma fibers on the top

Notes: Fig. 3a and 3b are morphological images of the sclerenchyma fibers on the top at the moment of 0 and 6 min upon loading.

Stretched Parenchymatous Tissues at the Bottom

Two kinds of crack propagation paths are presented in Fig. 4. The initial microcrack occurred in the parenchymatous cells because they were subjected to tensile stress at the bottom. The parenchymatous tissues experienced a perforated tear along the loading direction, and horizontal crack transmission began when the perforated tear reached the fibers, which then presented two crack growth paths. For one case, the crack thoroughly propagated along the fibrous length direction, and another stretching process of the sclerenchyma cells was observed (Fig. 4a). In Fig. 4b, the crack propagated between the fibers until a weak load-bearing point appeared, and then it expanded up through the parenchymatous groups. As a whole, the cracks formed with a ladder-like growth, and propagation paths were not restricted to just a coherent one, which implies that both the tensile and shear stresses caused the failure of the bamboo during the bending process (Obataya *et al.* 2007).

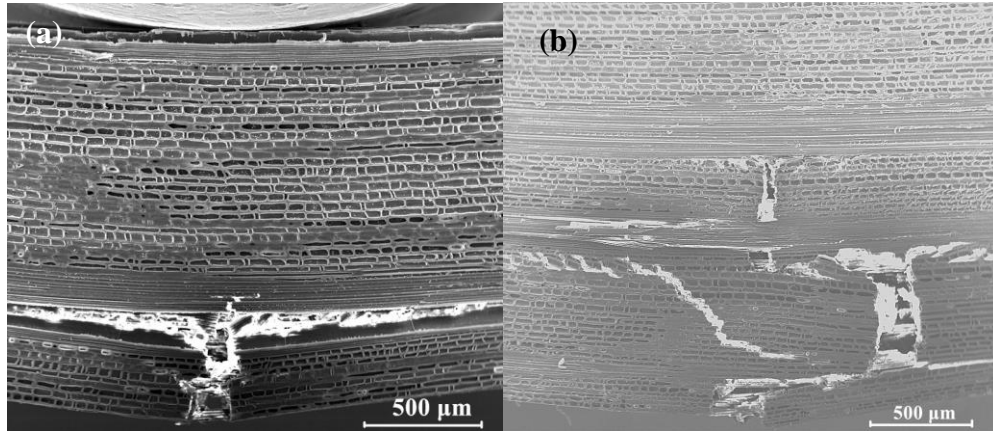


Fig. 4. Stretched parenchymatous tissues at the bottom

Notes: Fig. 4a and 4b are morphological images of the stretched parenchymatous tissues at the bottom for two separated specimens near failure point.

Stretched Sclerenchyma Fibers at the Bottom

To investigate whether sclerenchyma fibers were distributed at the bottom, the failure mode of the bamboo sliver under flexural stress is illustrated in Fig. 5.

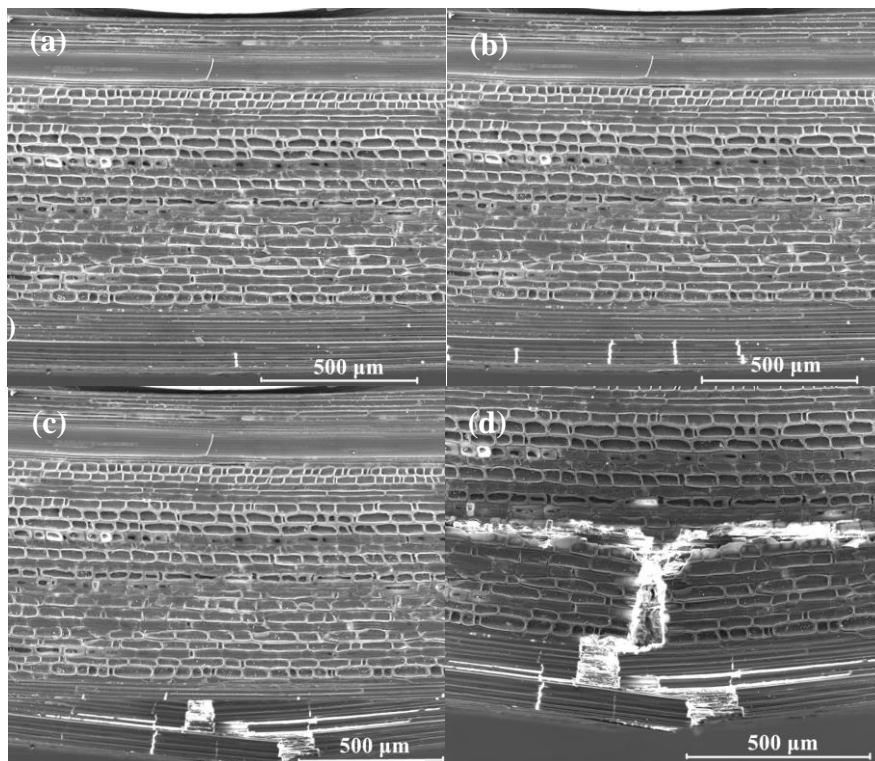


Fig. 5. Stretched sclerenchyma fibers at the bottom

Notes: Fig. 5a, 5b, 5c, and 5d are morphological images of the stretched sclerenchyma fibers at the bottom for one specimen at the moment of 0, 7, 10 and 15 min upon loading.

Initial microcrack development occurred on the bottom fibers because they were subjected to tensile stress (Fig. 5a), while the other fibers continued to be stretched until several fibrous tensile failure cracks were observed (Fig. 5b). The crack began horizontal

transmission when it reached the section between the fibers, and then it expanded upwards following the tensile failure of another group of fibers (Fig. 5c), which implied that the sclerenchyma fibers provided bamboo with a deformation resistance for its flexural ductility. As tensile and flexural load increased, the crack reached the parenchymatous tissues, which suffered a perforated tear along the loading direction (Fig. 5d). In general, the failure mode of the bamboo sliver in this section was similar to the case in Fig. 4.

CONCLUSIONS

1. The morphological behavior of bamboo was investigated through *in-situ* observation during the bending process, with respect to its fiber-foam composite observation. The parenchymatous tissues and sclerenchyma fibers made different contributions to the overall flexural ductility of bamboo. Sclerenchyma fibers supplied a deformation resistance, while parenchymatous tissues offered deformation space for the allowance of macroscopic deformation.
2. Parenchymatous tissues and sclerenchyma fibers are present in bamboo in a certain proportion, and reached their breakage point separately, which implied the alternation of stress concentration and relief. The unique combination of parenchymatous tissues and sclerenchyma fibers led to a functional gradient structure that showed bamboo regulating energy absorption and release, and accommodating itself to a complicated natural environment.

ACKNOWLEDGMENTS

The authors gratefully acknowledge financial support from National 13th Five-year “Major R&D Plan Project” (2016YFD0600904; 2016YFD0600905). The constructive comments from the anonymous reviewers are also greatly appreciated.

REFERENCES CITED

- Abe, K., and Yano, H. (2010). “Comparison of the characteristics of cellulose microfibril aggregates isolated from fiber and parenchyma cells of moso bamboo (*Phyllostachys pubescens*),” *Cellulose* 17(2), 271-277. DOI: 10.1007/s10570-009-9382-1
- Aizenberg, J., Weaver, J. C., Thanawala, M. S., Sundar, V. C., Morse, D. E., and Fratzl, P. (2005). “Skeleton of *Euplectella* sp.: Structural hierarchy from the nanoscale to the macroscale,” *Science* 309(5732), 275-278. DOI: 10.1126/science.1112255
- Fratzi, P., and Weinkamer, R. (2007). “Nature’s hierarchical materials,” *Progress in Materials Science* 52(8), 1263-1334. DOI: 10.1016/j.pmatsci.2007.06.001
- Jiang, Z. (2007). *Bamboo and Rattan in the World*, China Forestry Publishing House, Beijing, China.
- Liese, W. (1987). “Research on bamboo,” *Wood Science and Technology* 21(3), 189-209. DOI: 10.1007/BF00351391
- Long, L., Wang, Z., and Chen, K. (2015). “Analysis of the hollow structure with functionally gradient materials of moso bamboo,” *Journal of Wood Science* 61(6), 569-577. DOI: 10.1007/s10086-015-1504-9

- Obataya, E., Kitin, P., and Yamauchi, H. (2007). "Bending characteristics of bamboo (*Phyllostachys pubescens*) with respect to its fiber-foam composite structure," *Wood Science and Technology* 41(5), 385-400. DOI 10.1007/s00226-007-0127-8
- Shao, Z. P., Fang, C. H., Huang, S. X., and Tian, G. L. (2010). "Tensile properties of moso bamboo (*Phyllostachys pubescens*) and its components with respect to its fiber-reinforced composite structure," *Wood Science and Technology* 44(4), 655-666. DOI: 10.1007/s00226-009-0290-1
- Xian, Y., Chen, F., Li, H., Wang, G., Cheng, H., and Cao, S. (2015). "The effect of moisture on the modulus of elasticity of several representative individual cellulosic fibers," *Fibers and Polymers* 16(7), 1595-1599. DOI: 10.1007/s12221-015-5079-2
- Yu, Y., Wang, H., Lu, F., Tian, G., and Lin, J. (2014). "Bamboo fibers for composite applications: A mechanical and morphological investigation," *Journal of Materials Science* 49(6), 2559-2566. DOI: 10.1007/s10853-013-7951-z

Article submitted: March 3, 2018; Peer review completed: April 30, 2018; Revised version received and accepted: May 7, 2018; Published: May 25, 2018.
DOI: 10.15376/biores.13.3.5472-5478